Bayesian network modelling of phosphorus pollution in agricultural catchments with high-resolution data

Environmental Modelling and Software 178 (2024) 106073

Contents lists available at ScienceDirect

Environmental Modelling and Software

journal homepage: www.elsevier.com/locate/envsoft

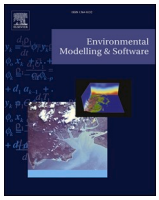

Bayesian network modelling of phosphorus pollution in agricultural catchments with high-resolution data

Camilla Negri [a,b,c,d,*], Per-Erik Mellander [a], Nicholas Schurch [d], Andrew J. Wade [c], Zisis Gagkas [b], Douglas H. Wardell-Johnson [b], Kerr Adams [b], Miriam Glendell [b]

[a] Agricultural Catchments Programme, Teagasc Environment Research Centre, Johnstown Castle, Co. Wexford Y35 Y521, UK
[b] The James Hutton Institute, Craigiebuckler, Aberdeen AB15 8QH, UK
[c] University of Reading, School of Archaeology, Geography and Environmental Science, Whiteknights, Reading, RG6 6AB, UK
[d] Biomathematics and Statistics Scotland, Craigiebuckler, Aberdeen AB15 8QH, UK

ARTICLE INFO

Handling Editor: Daniel P Ames

Keywords:
Diffuse pollution
Point sources
High-resolution water-quality monitoring
Participatory model
Uncertainty

ABSTRACT

A Bayesian Belief Network was developed to simulate phosphorus (P) loss in an Irish agricultural catchment. Septic tanks and farmyards were included to represent all P sources and assess their effect on model performance. Bayesian priors were defined using daily discharge and turbidity, high-resolution soil P data, expert opinion, and literature. Calibration was done against seven years of daily Total Reactive P concentrations. Model performance was assessed using percentage bias, summary statistics, and visually comparing distributions. Bias was within acceptable ranges, the model predicted mean and median P concentrations within the data error, with simulated distributions more variable than the observations. Considering the risk of exceeding regulatory standards, predictions showed lower P losses than observations, likely due to simulated distributions being left-skewed. We discuss model advantages and limitations, the benefits of explicitly representing uncertainty, and priorities for data collection to fill knowledge gaps present even in a highly monitored catchment.

1. Introduction

Phosphorus (P) losses from farmland to surface waters (diffuse P losses) continue to be a major cause of water quality deterioration and eutrophication (European Environment Agency, 2019). P remains a major source of water quality failures in Ireland, particularly due to the slow release of soil legacy P (Schulte et al., 2010), which is often unaccounted for in soil P tests (Thomas et al., 2016b). There are multiple challenges facing land managers, stakeholders, and policymakers when tackling P pollution in agricultural catchments in Northwest Europe (Bol et al., 2018). Smaller catchments (<50 km^2) vary in their vulnerability to P losses, necessitating a catchment-specific understanding of stressor-impact relationships and targeting of mitigation measures (Glendell et al., 2019). Drivers of P transfer differ across spatial scales (point, plot, field, hillslope, and catchment), and the understanding gained from laboratory or field measurements may not be directly applicable at the catchment scales represented in models (Brazier et al., 2005; Wade et al., 2008). Additionally, the understanding of key drivers of catchment vulnerability is complicated by different P sources and pathways that result in similar concentration-discharge hysteresis relationships at the catchment outlet. This confounding often makes it difficult to determine the most important P sources and pathways to target with P reduction measures and to predict their likely effect (Bol et al., 2018).

Soil P content and excess plant available P, derived from fertilizer application, have been identified as the main sources of diffuse P in Irish agricultural catchments (Regan et al., 2012), while some studies stress the importance of point pollution sources (Campbell et al., 2015; Gill and Mockler, 2016; Vero et al., 2019) as well as legacy P (Thomas et al., 2016b). In addition, the transport and delivery of P in Irish agricultural catchments are dominated by weather and hydrological conditions rather than initial soil P (Mellander et al., 2015, 2018). To investigate diffuse P pollution sources in Irish agricultural catchments, modelers have used two main approaches: 1) the critical source areas (CSAs) approach (Packham et al., 2020; Thomas et al., 2016b, 2021), and 2) the load apportionment approach (Crockford et al., 2017; Mockler et al., 2017). CSAs methods aim at identifying and mapping areas of high hydrological activity connected with areas of elevated P mobilisation,

* Corresponding author. The James Hutton Institute, Craigiebuckler, Aberdeen AB15 8QH, Scotland UK.
E-mail address: camilla.negri@hutton.ac.uk (C. Negri).

https://doi.org/10.1016/j.envsoft.2024.106073
Received 13 November 2023; Received in revised form 7 May 2024; Accepted 10 May 2024
Available online 13 May 2024

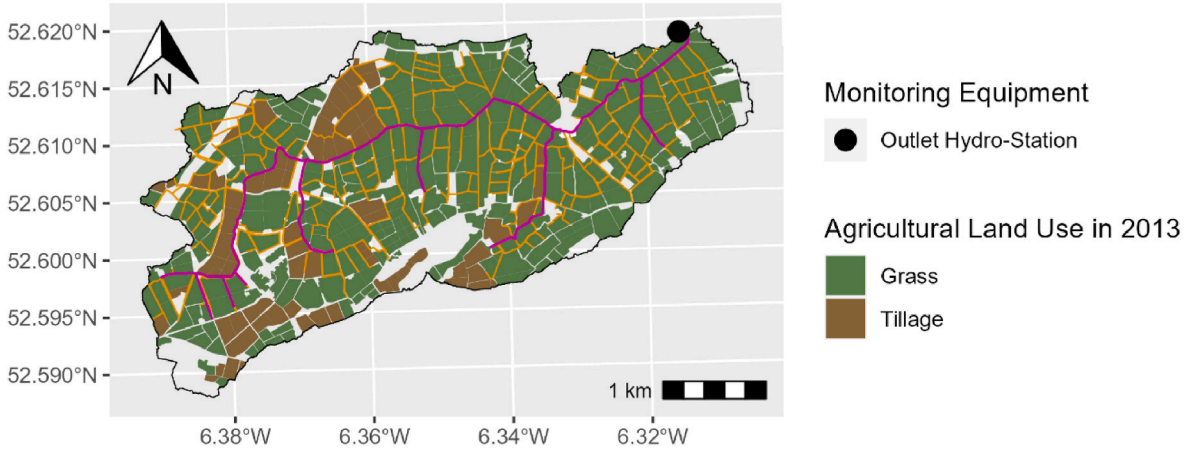

Fig. 1. Study area: the Ballycanew catchment in County Wexford. Elevation varies between 21 m a.s.l. And 232 m a.s.l. The location of the hydrometric station is marked with the black dot, while magenta lines represent streams and yellow lines represent artificial drainage.

thus facilitating the transfer of P from terrestrial to aquatic ecosystems (Djodjic and Markensten, 2019). One of the biggest advantages of CSAs is that they provide the basis to spatially identify potential locations for mitigation measures, however, these approaches require extensive sampling and mapping of P sources and hydrological connectivity, and provide qualitative results that might be difficult to interpret for policy, to validate, or evaluate at larger scales (Djodjic and Markensten, 2019). In contrast, Load Apportionment Models (LAMs), calculate nutrient loads from all sources and then estimate factors to reduce such loads to account for treatment (e.g. wastewaters) or environmental attenuations. Estimated loads are then compared with loads calculated from measurements (Mockler et al., 2016). This method can identify the dominant pollution contributors in catchments and sub-catchments, while also assessing management strategies (Mockler et al., 2016). However, LAMs can be difficult to interpret for non-experts, because of the uncertainties around load estimation, especially when used with low-frequency datasets, which limits their utility as management tools (Crockford et al., 2017).

Catchment nutrient models are crucial to summarize current knowledge and process understanding, as well as to test land use and climate scenario effects on water quality, which can inform mitigation action (Jackson-Blake et al., 2015). However, mechanistic models of water quality (e.g. catchment scale P models like INCA-P (Jackson-Blake et al., 2016),), can have parameters that are unmeasurable yet heavily influence model outputs (Jackson-Blake et al., 2017) and are often over-parameterized, especially when upscaling to watershed scales (Radcliffe et al., 2009). Additionally, P models often perform inadequately in rural catchments where diffuse sources are dominant, and model outputs' accuracy is limited by current knowledge (Jackson-Blake et al., 2015). Furthermore, water quality and nutrient transport models are frequently hindered by constraints associated with available data, the presence of non-linear interactions, and temporal and spatial scale representation issues (Blöschl et al., 2019; Harris and Heathwaite, 2012; Rode et al., 2010; Wellen et al., 2015). Hence, there is a recognition of the importance of incorporating uncertainty explicitly in hydrological and water quality modelling, not only through error bounds on output values, but by representing uncertainty as an intrinsic aspect of inexact environmental science (Beven, 2019; Pappenberger and Beven, 2006). Additionally, given the high levels of uncertainty and complexities involved in water quality mitigation and modelling, there is a pressing need to develop and apply probabilistic modelling tools for Environmental Risk Assessment (ERA) as an alternative to deterministic methods, and Bayesian Belief Networks (BBNs) are particularly well suited for this purpose (Moe et al., 2021). BBNs are a probabilistic graphical modelling framework that represents a set of variables and their conditional dependencies using a Directed Acyclic Graph (DAG) i.e., a network that has no cycles. BBNs are a powerful tool for modelling complex systems and have been used to integrate the disparate physicochemical, biotic/abiotic, and socio-economic aspects (Penk et al., 2022) needed to simulate P in river catchments (Jarvie et al., 2019). BBNs show promise as decision support tools in water resource management (Phan et al., 2019) because they represent causal relationships between variables transparently and graphically, making it straightforward to understand and build BBNs with the participation of experts. BBNs facilitate an improved understanding of risk by explicitly representing the uncertainties and assumptions in the model as probability distributions, and they provide a systems-level understanding of a problem (Aguilera et al., 2011; Barton et al., 2012; Forio et al., 2015; Glendell et al., 2022; Kaikkonen et al., 2021; Kragt, 2009; Uusitalo, 2007). BBNs' can make predictions with sparse data (Forio et al., 2015; Glendell et al., 2022; Uusitalo, 2007); and the probabilistic outputs from BBNs can be used to recommend actions to policy makers, and to communicate best practices to stakeholders (Barton et al., 2012; Kaikkonen et al., 2021; Uusitalo, 2007). The probability distributions used in BBNs represent (most) model parameters explicitly encoding the uncertainties in the prior knowledge, data, and parameters (Sahlin et al., 2021). These prior distributions can be assumed, elicited from expert knowledge, or quantified using prior data. However, hybrid Bayesian Networks (BBNs that have a combination of continuous and discrete variables) are rarely applied in water quality modelling, and they have not been tested in a catchment with high-resolution monitoring data. Glendell et al. (2022) found that a hybrid BBN developed using standard regulatory data in seven test catchments in Scotland performed well, albeit with relatively large predictive uncertainty. In this work, we test whether a hybrid BBN can perform better when applied and calibrated in a catchment with long-term high-resolution data to understand whether the wide predictive uncertainty can be reduced or whether it is an irreducible property of this stochastic modelling approach. Hence, in this study we developed a BBN model of in-stream P concentrations in a poorly drained Irish agricultural catchment to: (1) model P losses in a data-rich meso-scale agricultural catchment using high-resolution observational data and expert advice; (2) evaluate the impact of rural point sources (septic tanks and farmyards), which are seldom represented in catchment water quality models, on P losses, and (3) evaluate the strengths and weaknesses of using BBNs as a modelling framework for high-resolution observational hydrological data.

2. Materials and methods

2.1. Study area

This study focusses on the Ballycanew catchment (in older papers,

Table 1
Model specifications organized by sub-model. The "Hydrology", "Management", and "Soil erosion and soil P" sub-models belong to both Model A and B (Delignette-Muller et al., 2020; Environmental Protection Agency Ireland (EPA), 2000, Environmental Protection Agency Ireland (EPA), 2003, Environmental Protection Agency Ireland (EPA), 2015; Gill, 2005; Gill et al., 2007; Shore et al., 2016; Wall et al., 2012; Stutter et al., 2021).

Variable (symbol) [unit]	States	Discretisation boundaries/ Probability	Description
Hydrology sub-model (Drivers)			
Month	Each month		Calculated as No. days in the month/ 365
Calculated variables			
Mean total monthly Q (discharge) [m^3]	Very Low	0-109424	Bootstrapped from daily total discharge observations (2009-2016) to obtain a Lognormal (μ; σ) discharge distribution with base e for each month. Each month's parameters are shown in the table. Discretization of states is based on percentiles calculated from the average monthly observations (very low<= 5th percentile, low= 5th-25th percentile, medium= 25th-50th percentile, high= 50th-75th percentile, very high= 75th-100th percentile).
	Low	109424-227082	
	Medium	227082-373942	
	High	373942-806788	
	Very High	806788-1124380	
Mean total monthly Surface Flow (surface runoff) [m^3]	Very Low	0-28450	Calculated as a portion of mean monthly runoff (26%), via hydrograph separation method described in Mellander et al., (2012). Discretization of states is based on percentiles calculated from observations (very low<= 5th percentile, low= 5th-25th percentile, medium= 25th-50th percentile, high= 50th-75th percentile, very high= 75th-100th percentile).
	Low	28450-59042	
	Medium	59042-97225	
	High	97225-209765	
	Very High	209765-292338	
Mean total monthly Sub-surface Stormflow (subsurface runoff) [m^3]	Very Low	0-19696	Calculated as a portion of mean monthly runoff (18%), via hydrograph separation method described in Mellander et al., (2012). Discretization of states is based on percentiles calculated from observations (very low<= 5th percentile, low= 5th-25th percentile, medium= 25th-50th percentile, high= 50th-75th percentile, very high= 75th-100th percentile).
	Low	19696-40875	
	Medium	40875-67309	
	High	67309-145222	
	Very High	145222-202388	
Mean total monthly Baseflow [m^3]	Very Low	0-61277	Calculated as a portion of mean monthly runoff (56%), via hydrograph separation method described in Mellander et al., (2012). Discretization of states is based on percentiles calculated from observations (very low<= 5th percentile, low= 5th-25th percentile, medium= 25th-50th percentile, high= 50th-75th percentile, very high= 75th-100th percentile).
	Low	61277-127166	
	Medium	127166-209407	
	High	209407-451801	
	Very High	451801-629651	
Management (Drivers)			
Land use	Arable	0.20	As reported by Teagasc - Agriculture and Food Development Authority, (2018).
	Grassland	0.78	
	Seminatural	0.02	
Buffers			Buffer strips are defined as being 2 m in width, more than 2 m in width, or absent. Probabilities of having either type of buffer according to land use were agreed upon with one of the ACP advisors (expert) during consultation.
Calculated variables			
Buffer effectiveness for Particulate P (PP) and suspended sediments (SS)	Very Low	0-0.2	Dependent on the variable Buffers. For 2 m buffers, effectiveness is defined as Beta (α=2.9; β=4.5); for >2 m buffers it is defined as Beta (α=1.44; β=0.789); for no buffers, effectiveness is equal to 0. The distributions were fitted to the dataset published in Stutter et al., (2021), where negative retention data was deleted from the analysis.
	Low	0.2-0.4	
	Medium	0.4-0.6	
	High	0.6-0.8	
	Very High	0.8-1	
Buffer effectiveness for Total Dissolved P (TDP)	Very Low	0-0.2	Dependent on the variable Buffers. For Buffers 0-2 m, Buffer effectiveness is defined as Beta (α=1.8; β=2.7), for >2 m buffers it is defined as Beta (α=1; β=0.8); for no buffers, effectiveness is equal to 0. The distributions were fitted to the dataset published in Stutter et al., (2021), where negative retention data was deleted from the analysis.
	Low	0.2-0.4	
	Medium	0.4-0.6	
	High	0.6-0.8	
	Very High	0.8-1.0	
Soil erosion and soil P sub-model			
Morgan P			Based on land use, proportions of land for each level and in each land use category were calculated

	μ	σ
January	13.8	0.17
February	13.5	0.18
March	12.9	0.17
April	12.5	0.19
May	12.2	0.21
June	11.8	0.30
July	11.3	0.32
August	11.8	0.50
September	11.5	0.36
October	12.8	0.40
November	13.7	0.21
December	13.8	0.21

Land use	Arable	Grassland	Seminatural
2 m	0.98	0.1	$1.01*10^{-6}$
>2 m	0.019	0.1	$1.01*10^{-6}$
none	0.001	0.8	0.999

	Arable	Grassland	Seminatural
Morgan1	0.40	0.46	0

		Morgan2	0.49	0.35	0.6
		Morgan3	0.09	0.14	0.3
		Morgan4	0.02	0.05	0.1
					based on the soil survey carried out in 2013 in the catchment. Where the Morgan P index was unknown, that proportion of land was assigned to the dominant index category. For the interpretation of the Soil Morgan P Index, the reader is referred to Regan et al., (2012).
Calculated variables					
Monthly Turbidity [NTU month^{-1}]	Very Low	0-1402			Bootstrapped from daily average turbidity observations (2009-2016) to obtain a Lognormal (μ; σ) turbidity distribution with base e for each month. Each month's parameters are shown in the table. Discretization of states is based on percentiles calculated from the average monthly observations (very low<= 5th percentile, low= 5th-25th percentile, medium= 25th-50th percentile, high= 50th-75th percentile, very high= 75th-100th percentile).
	Low	1402-1665			
	Medium	1665-2270			
	High	2270-3391			
	Very High	3391-4344			

	μ	σ
January	6.3	0.25
February	6.0	0.23
March	5.6	0.23
April	5.5	0.20
May	5.3	0.15
June	5.5	0.15
July	5.2	0.13
August	5.2	0.13
September	5.2	0.12
October	5.7	0.24
November	6.2	0.30
December	6.2	0.30

Monthly Suspended Sediment concentration [mg l^{-1} month^{-1}]	Very Low	0-133.3	Calculated as: a * Monthly Turbidity [NTU month^{-1}] ^{b}, where a= 0.567, and b= 1.1109, as described in Sherriff et al., (2015). Discretization of states is based on percentiles calculated from the average monthly calculated observations (very low<= 5th percentile, low= 5th-25th percentile, medium= 25th-50th percentile, high= 50th-75th percentile, very high= 75th-100th percentile).
	Low	133.3-165	
	Medium	165-237.6	
	High	237.6-369.3	
	Very High	369.3-480.0	
Water Extractable P (WEP) [mg l^{-1}]	Low	0-3	Based on variable "Morgan P levels" and "land use" (data from 2013) it is calculated with the equations available in (Thomas et al., 2016b): for Grassland, WEP=0.60 * Morgan P + 1.46, for Arable: WEP= 0.45 * Morgan P + 0.19, where Morgan P is defined as a Uniform distribution with the following parameters:
	Medium	3-5	
	High	5-8	
	Very High	8-15	

Morgan P Index	**Grassland**	**Arable**
Index 1	a=0; b=3	a=0; b=3
Index 2	a=3.1; b=5	a=3.1; b=6
Index 3	a=5.1; b=8	a=6.1; b=10
Index 4	a=8.1; b=30	a=10.1; b=30

For the Seminatural Land use, WEP was assumed constant to 0.001. Discretization is based on Morgan P discrete levels.

Sediment Water Soluble P [mg kg^{-1}]	Very Low	0-0.0995	Defined as a Lognormal distribution (μ=-0.9, σ=1), fitted with the *SHELF* R package version 1.8.0, (Oakley, 2020) to observed Water Extractable P in the catchment sediments (Shore et al., 2016). Discretization of states is based on percentiles calculated from the observations (very low<= 5th percentile, low= 5th-25th percentile, medium= 25th-50th percentile, high= 50th-75th percentile, very high= 75th-100th percentile).
	Low	0.0995-0.2100	
	Medium	0.2100-0.3550	
	High	0.3550-0.9100	
	Very High	0.9100-8	
Predicted Dissolved P Concentration [mg l^{-1}]	Low	0-3	Dependant on Water Extractable P, it is defined with the linear model: Predicted Dissolved P = β(WEP)+α, where β =0.08, α =0.158, derived from (Thomas et al., 2016b). This equation is derived from data gathered during the closed period only, that is, when farmers are forbidden from spreading fertilizer. An assumption is made that when the linear model yields a negative value, that is resampled as a zero. Water Extractable P is considered a good in-stream TRP/ TDP predictor in the ACP catchments by the experts, however careful consideration is needed when choosing a soil P test in a different setting.
	Medium	3-5	
	High	5-8	
	Very High	8-15	
Sub-surface Dissolved P load [kg month^{-1}]	Low	0-3	Calculated as the product of Predicted Dissolved P concentration and Subsurface Storm-flow.
	High	3-200	
Baseflow Dissolved P load	Low	0-3	Calculated as the product of Predicted Dissolved P

[kg month^{-1}]	High	3-200	concentration and Baseflow.
Modified Dissolved P load [kg month^{-1}]	Low	0-3	Based on "Buffer effectiveness for Total Dissolved P", for effective buffers, modified Dissolved P load= Sub-surface Dissolved P load *(1-Buffer effectiveness for TDP). Based on expert recommendation.
	High	3-200	
Monthly Sediment P load [kg month^{-1}]	Low	0-3	Calculated as the product of Sediment Water Soluble P [mg kg^{-1}], Monthly Suspended Sediment concentration [mg l^{-1} month^{-1}], and Mean total monthly surface flow [m^3] .
	High	3-200	
Modified Sediment P load [kg month^{-1}]	Low	0-3	Based on "Buffer effectiveness for Suspended Sediments and Particulate P", for effective buffers, Modified Sediment P load= Monthly Sediment P load [kg month^{-1}]*(1-Buffer effectiveness for SS and PP). Based on expert recommendation.
	High	3-200	
Septic Tanks (ST) sub-model (Point P sources), included in Model B only			
P concentration per tank [mg l^{-1}]	Absent (to represent 0 STs)	0-1*10^{-8}	P concentration is dependent on the treatment type. If the treatment is unknown, the concentration is defined as a Lognormal distribution (μ=2.9, σ =1.25), based on a literature review of data available for Ireland (Environmental Protection Agency Ireland (EPA), 2003, 2000; Gill et al., 2005, 2007) (n=8). Fitting was done with R package *fitdistrplus* version 1.1-8, (Delignette-Muller et al., 2020). Otherwise, for primary and secondary treatment concentration is defined as Truncated Normal distribution (μ=10; σ=1), and (μ=5; σ=0.5) respectively, as described in Glendell et al., (2021) and derived from SEPA guidelines (Brownlie et al., 2014). All tanks are assumed to be maintained. Discretization was also based on the literature review.
	Low	1*10^{-8}-1	
	Medium	1-18	
	High	18-35	
	Very High	35-100	
Management related variables			
Direct discharge	Present	0.16	Probabilities are derived from the Environmental Protection Agency Ireland (EPA, 2015).
	Absent	0.84	
Treatment	Unknown	0.50	Probability of having "unknown", "primary" or "secondary" treatment of the effluent in a septic tank. Probabilities based on a survey conducted within WaterProtect, a research project supported by the European Union research and innovation funding programme Horizon 2020 [grant no. 727450].
	Primary	0.31	
	Secondary	0.19	
Connectivity related variables			
Degree of Phosphorus Saturation (DPS) [%]	Very Low_0_20	0.978	Discretization is equal to the 20th, 40th, 60th, and 80th quantiles, however 0< DPS <60 in this catchment. Probabilities were calculated from available spatial data (Wall et al., 2012).
	Medium_20_40	0.017	
	High_40_60	0.005	
Soil risk factor [adimensional]	Very Low	9.9*10^{-6}	An indicator to describe the combined risk of effluent leaching to the groundwater table with the risk of the effluent being transported with surface runoff. This approach is a simplification of the one adopted in Glendell et al., (2021). The risk factor was obtained by overlaying the soil series (Thomas et al., 2016a) with information on the position of the groundwater table (0- 2 m below ground or more than 2 m below ground). Because little is known regarding the septic tanks in the catchment (i.e. age, type of treatment, maintenance), and the groundwater table position (few datapoints within the catchment) experts recommended a precautionary principle. This meant that the class at most risk of effluent transfer was applied when data was unavailable. The table to the left represents a synthesis of the classification approach. Probabilities are based on land cover proportion.
	Low	0.374	
	Medium	9.9*10^{-6}	
	High	0.620	
	Very High	0.006	

	Groundwater Table Position	
Soil Series	**0-2 m below surface**	**>2 m below surface**
Brown earths	High Risk	Moderate Risk
Alluvial	High Risk	Moderate Risk
Luvisol	High Risk	Moderate Risk
Gley	Very High Risk	Very High Risk

Soil risk factor	**DPS**	**Low**	**Medium**	**High**
Very low	**Very Low**	0.0	0.0	1.0
	Medium	0.0	0.5	0.5
	High	0.5	0.5	0.0
Low	**Very Low**	0.0	0.3	0.7
	Medium	0.0	0.7	0.3
	High	0.3	0.7	0.0
Medium	**Very Low**	0.0	0.5	0.5
	Medium	0.0	1.0	0.0
	High	0.5	0.5	0.0
High	**Very Low**	0.0	0.7	0.3
	Medium	0.3	0.7	0.0
	High	0.7	0.3	0.0
Very High	**Very Low**	0.0	0.5	0.5

Leachfield removal — The node refers to P removal from septic drains. Conditional on P leaching risk from Degree of Phosphorus Saturation (DPS). The conditional probability table is a logical one.

	Medium	0.5	0.5	0.0	
	High	1.0	0.0	0.0	

Leachfield connectedness

HSA rescaled	None		Low		Medium		High	
Direct discharge	pres	abs	pres	abs	pres	abs	pres	abs
low	0	1	0	1	0	0	0	0
medium	0	0	0	0	0	1	0	0
high	1	0	1	0	1	0	1	1

Probabilities are conditional on the presence/absence of Direct ST discharge, and HSA (node: Connectivity rescaled HSA). Where Direct discharge is present, connectedness is assumed as 'high'. Where Direct discharge is absent, the risk class of the HSA is assigned.

Septic Tank connectedness

Leachfield removal	Low			Medium			High		
Leachfield connectedness	Low	Medium	High	Low	Medium	High	Low	Medium	High
Low	1.0	0.0	0.0	1.0	0.0	0.0	1.0	0.5	0.0
Medium	0.0	1.0	0.0	0.0	1.0	0.5	0.0	0.5	1.0
High	0.0	0.0	1.0	0.0	0.0	0.5	0.0	0.0	0.0

Probabilities are conditional on Leachfield removal and Leachfield connectedness. Where Leachfield removal is 'low' or 'High', Leachfield connectedness remains unaltered.

Connectivity rescaled HSA [adimensional]	None_0	0.60
	Low_1_3	0.18
	Medium_4_7	0.20
	High_8_10	0.02

Data extracted from spatial layers of Hydrologically Sensitive Areas (HSAs) rescaled between 0 and 10 was provided by the Agricultural Catchments Programme (Thomas et al., 2016b). Discretization is also based on the spatial layers.

Calculated variables

Load per tank [kg month^{-1}]	Absent	0-1*10^{-6}
	Very Low	1*10^{-6}-0.1
	Low	0.1-0.5
	Medium	0.5-1.0
	High	1.0-2.0
	Very High	2.0-30

Specified as the product of ST density [No ha^{-1}] * ST concentration [mg l^{-1}] * 120 [L] average daily water consumption per person * 365/12 days in a month* average No of persons per household 2.7/1*10^{6}. Discretisation is based on interpolation to represent plausible probabilities for combination of extreme risk classes (eg. High+high=high, low+low=low).

Total Realized load [T month^{-1}]	Very Low	0.0-0.1
	Low	0.1-0.5
	Medium	0.5-1.0
	High	1.0-2.0
	Very High	2.0-12

Septic tank connectedness	Delivery factor (D)	Reference

Calculated as the product of septic tank load and delivery factors (D) related to the connectedness of a septic tank, based on the median estimated fraction to be delivered in Table 13 of the report by Glendell et al., (2021) and the number of septic tanks present within catchment boundary (N): Realised load per tank [kg month^{-1}] * N * D / 1000. In this case, N= 88. Discretisation based on interpolation to represent plausible probabilities for

also referred to as Grassland B, for example in Sherriff et al. (2015), Fig. 1) located near Gorey, County Wexford, Ireland. The catchment covers 1207 ha and is comprised of 78% grassland and 20% tillage land use, while the remainder 2% is considered seminatural land use (Table 1). The catchment has been monitored intensively as part of the Agricultural Catchments Programme (ACP), Teagasc (Wall et al., 2011), which started in 2009 and is ongoing. Ballycanew soils have poor drainage characteristics due to deposits of heavy clays. However, landowners in the area have improved the land for grass production with tile and mole drainage. The low soil permeability in the catchment results in flashy hydrology and a high risk of P loss to water through quick and erosive surface pathways during heavy rain events (Mellander et al., 2015).

2.2. Data collection

2.2.1. Hydrochemistry

The Ballycanew catchment is equipped with a river bank-side kiosk where the instrumentation is installed, its location is marked in Fig. 1 as Outlet Hydro-Station (Mellander et al., 2012; Jordan et al., 2007). River water level is recorded every 10 min in a stilling well in the catchment outlet using an OTT Orpheus Mini vented-pressure instrument. The river discharge is calculated from a rating curve developed in a flat-V weir using an Acoustic Doppler Current meter. Total phosphorus (TP) and total reactive phosphorus (TRP) concentrations are monitored with a Hach-Lange Phosphax within the range of 0.01–5.00 mg l^{-1}, co-located with a Solitax Hach-Lange turbidity (turbidity units, NTU, also recorded every 10 min) sensor field-calibrated to suspended sediment concentration (mg l^{-1}) (Sherriff et al., 2016).

Data from the bank-side monitoring station (Fig. 1, Outlet Hydro-Station) collected every 10 min (total discharge, average total reactive P concentrations, and average turbidity), were aggregated to daily average values for this study.

2.3. Bayesian Belief Network development

Bayesian Networks are directed acyclic graphs (DAGs), that represent a set of variables and their conditional dependencies using a graphical model. The term "directed acyclic" means that there is a sequential flow of information among variables and no dynamic feedback loops (Barton et al., 2012; Kragt, 2009). An introduction to Bayesian Networks and their application in ERA can be found in Moe et al. (2021), and won't be repeated here. The relationships between variables in a BBN are parameterized using conditional probability distributions or conditional probability tables when variables are discrete (CPTs), and the graphical network is a description of such relationships (Borsuk et al., 2004). A hybrid Bayesian network combines both discrete and continuous variables, the latter represented as probability distributions. In this study, a conceptual BBN was developed in GeNIe 2.4 (BayesFusion, 2019) visualizing the 'source-mobilisation--transport-continuum' (Haygarth et al., 2005) and identifying the main drivers of phosphorus pollution in the catchment. The initial DAG comprised of 63 nodes and 81 arcs, with 325 independent parameters out of 483, with parameter count defined as the total size of CPTs while independent parameters are those not implied by other parameters. The average number of node parents (indegree) was 1.3, and the maximum number of node parents was 5. An extensive literature review was conducted summarizing the knowledge base for the subject which was used to inform the priors (distribution shapes and parameter values) for key parameters in the models, as shown in Table 1. Catchment-specific information was also collated and used to inform the model structure and priors (Appendix A).

From the initial parameterization, two models were developed: Model A, which only accounts for diffuse reactive P sources (i.e., losses

		Low	0.05	"very low" category in Appendix A3, Glendell et al., (2021)	combination of extreme risk classes.
		Medium	0.30	"medium" category in Appendix A3, Glendell et al., (2021)	
		High	0.80	"very high" category in Appendix A3, Glendell et al., (2021)	
Farmyards sub-model (Point P sources), included in Model B only					
Farmyard size area [m^2]	Very Low		0-56		Based on available farmyard survey, a distribution was fitted to farmyard area data: Lognormal (μ=-5.6; σ=0.98). Discretization of states is based on percentiles calculated from the observations (very low<= 5^{th} percentile, low= 5^{th}-25^{th} percentile, medium= 25^{th}-50^{th} percentile, high= 50^{th}-75^{th} percentile, very high= 75^{th}-100^{th} percentile).
	Low		56-127		
	Medium		127-277		
	High		277-586		
	Very High		586-4500		
Farmyard P concentration [mg l^{-1}]	Very Low		0-0.01		Using the *SHELF* R package (version 1.8.0, Oakley, 2020), a distribution was fitted to the data in Table 2 in Harrison et al., (2019): Lognormal (μ=-1.8; σ=1.6). The best fit would have been the LogT distribution, however, that is not available for GeNIe, so we opted for Lognormal. Discretization is also based on the literature. For simplicity, here we have used SRP to mean TRP.
	Low		0.01-0.50		
	Medium		0.50-1.00		
	High		1.00-2.50		
	Very High		2.50-60		
Incidental losses per average yard [kg $month^{-1}$]	Very Low		0-1*10^{-9}		Based on average farmyard size, losses are calculated as Surface runoff [m^3] / catchment area [m^2]* Farmyard size area [m^2]* Farmyard P concentration [mg l^{-1}]/ 10^3.
	Low		1*10^{-9}-0.001		
	Medium		0.001-0.01		
	High		0.01-0.10		
	Very High		0.10-60		
Total incidental losses [T $month^{-1}$]	Very Low		0-1*10^{-5}		Incidental losses per average yard [kg $month^{-1}$] * N, where N is the total number of yards present within the catchment boundary. In this case, N =70.
	Low		1e-05-0.007		
	Medium		0.007-0.070		
	High		0.07-0.700		
	Very High		0.700-10		
Catchment outlet integration sub-model					
Total catchment in-stream P load [T $month^{-1}$]	Low		0-0.02		Equal to the sum of Baseflow Dissolved P load [kg $month^{-1}$], Modified Dissolved P load [kg $month^{-1}$], Modified Sediment P load [kg $month^{-1}$], Total incidental losses [T $month^{-1}$], and Total Realized load [T $month^{-1}$], all converted to appropriate units.
	Medium		0.02-1		
	High		1-10		
In-stream P concentration [mg l^{-1}]	Good		0-0.035		Defined as the Total catchment in-stream P load [T] * 10^9 / Mean total monthly Q (discharge) [m^3] *
	Bad		0.035-10		
					1000, where mean monthly discharge is equal to the total catchment discharge measured at the outlet.
Environmental Quality Standard [TRP concentration mg l^{-1}]					Discretization of the variable "In-stream TRP concentration [mg l^{-1}]". For simplicity, in-stream TRP is here considered equal to in-stream Dissolved Reactive Phosphorus, as in previous studies the mean DRP accounted for 98–99% of the flow-weighted mean TRP (Shore et al., 2014).

TRP concentration	**Good**	**Bad**
Good	1	0
Bad	0	1

from soil matrix and topsoil), and Model B, which also includes P losses from farmyards, which is infrequent in P modelling (Harrison et al., 2019) and septic tanks, which are often overlooked as P sources, as opposed to centralized wastewater treatment centres (Withers et al., 2014). The models aim at integrating all the total reactive P losses from the different compartments at the catchment outlet ("Total catchment in-stream P load", T $month^{-1}$) and then converting the loads into concentrations (mg l^{-1}) by dividing by the monthly discharge (m^3 $month^{-1}$).

2.3.1. Expert input to inform key aspects of the model

Experts from the Agricultural Catchments Programme, the James Hutton Institute, and the Irish EPA with relevant areas of expertise (hydrology, hydrochemistry, land management, farm consultancy, policy making, and environmental modelling) were consulted in 1-to-1 meetings, and in a group workshop. Excluding the authors of this paper, whom we also consider part of the experts' pool, a total of thirteen experts were consulted, and their personal information anonymized. Before the interviews and workshops, experts were provided with a topic information sheet (available in Supplementary Information) describing the model and the aims and objectives of the session. The experts were asked to provide their input on the conceptual model structure to ensure that the causal dependencies between variables made sense and none were missing; parameterising variables and their relationships using equations; approving the CPT values for the "Buffers" (proportion of each type of buffer strip present in the catchment) node, as well as deciding which loads were impacted by the buffer reduction (i.e., only surface-pathway derived nodes); and were asked to provide recommendations for further information sources (e.g., reports, publications, or datasets).

2.4. Model structure

The model structure is presented in Fig. 2. The complete structure and specification of both models are included in Table 1 to allow reproducibility and further model application in different contexts. Table 1 describes the model structure and the conditional probability distributions and describes which CPTs were logical, contained expert judgement, and which were derived from data or literature, highlighting which sub-models and variables are part of Model A or Model B. In particular, the "Hydrology, "Management", and "Soil erosion and soil P" sub-models are represented in both Model A and B, while the sub-models "Septic Tanks" and "Farmyards" are only represented in Model B.

2.5. Model evaluation

P models typically struggle to produce positive performance indicators (Jackson-Blake et al., 2015). Additionally, BBNs cannot be evaluated with the traditional metrics used for hydrological models (for example, Nash-Sutcliffe Efficiency or Root Mean Square Error), because

Fig. 2. Structure of the final BBNs, including the additional nodes for Model B highlighted inside the box. The nodes in orange represent variables that pertain to Management, those in yellow represent Soil variables, those in turquoise represent the Hydrology variables, those in light blue represent the Turbidity-related variables, those in lilac represent the Loads within the catchment, and those in cyan represent the Concentrations integrated at the catchment outlet.

the number of observations does not correspond to the number of model realizations. Therefore, the model performance was evaluated following the procedures suggested by Jackson-Blake et al. (2015), using a suite of strategies comparing predicted TRP concentrations (mg l^{-1}) with the observed TRP concentrations (available as daily average, mg l^{-1}) (2009–10–01 to 2016–12–31) by 1) calculating percentage bias (PBIAS), 2) comparing summary statistics (median, mean, upper and lower limit, interquartile ranges), and 3) comparing the full posterior distributions with the observations. Using the R *SHELF* package (version 1.8.0, Oakley, 2020), a monthly lognormal distribution was fitted to the observed TRP concentrations using 100 quantiles and 0 as the lower limit. This distribution was used to compute the PBIAS % in the R package *hydroGOF* (version 0.4–0, Zambrano-Bigiarini, 2020). In addition, a bootstrapping method was applied to the available observations to obtain a lognormal distribution fitted to each month's TRP concentration data. Percentage bias was used to evaluate the BBNs performances in each month, in this case with 10,000 data points simulated in the BBNs by selecting each month as evidence, and 10,000 data points drawn from each month's lognormal distribution fitted to the observational data using bootstrapping. Both for the overall and the monthly performance evaluation, data points outside the instrument's limits of detection (0.01–5.00 mg l^{-1}) were excluded from the model evaluation.

3. Results and discussion

3.1. Model structure

As a result of the discussions with experts and the extensive data review, the final model versions (A and B) are considerably less complex than was initially conceptualized. As mentioned, the original BBN comprised 63 nodes and 81 arcs, while the resulting Model B comprises 38 nodes, 46 arcs, 106 independent parameters out of 153, average indegree of 1.2, and maximum indegree of 5. The original model structure (not shown here) included variables that were excluded from the final structure as a result of the consultations with experts. Fertilizer (organic plus inorganic) application based on stocking rates was excluded from the BBN as soil P fertilizer is applied only to maintain Morgan P levels, available at field scale. Erosion rates were also not included in the final version of the model as catchment-specific data was unavailable. Incidental losses due to animal poaching were also excluded as fencing of water courses is in place in the ACP catchments. The final BBN structure is shown in Fig. 2, which highlights which nodes were part of Model A and which ones were added for Model B. The model structure (Table 1) directly reports which variables were influenced by experts, in an attempt to address some of the transparency issues raised by Kaikkonen et al. (2021) regarding expert role.

3.2. Phosphorus concentrations

3.2.1. Phosphorus concentrations in the stream – overall performance

Overall model performance is shown in Table 2, where mean, lower and upper limit, and meaningful percentiles of the BBN TRP concentration distributions are shown against the average monthly distribution fitted to the observations. The 5th percentile shows that the model concentrations are more skewed towards low concentrations than the observations. This may be related to the equation used to calculate the variable "Predicted Dissolved P Concentration [mg l^{-1}]", reported in Table 1 and derived from Thomas et al. (2016b). The node was set up to substitute the negative values with zeroes as recommended by Thomas et al. (2016b). 25% of the simulated values for the "Predicted Dissolved P Concentration [mg l^{-1}]" node equalled zero (meaning no TRP from the soil matrix would be measured at the catchment outlet) and currently

Table 2
The two models' overall performances in terms of mean, standard deviation, quantiles, and percentage bias. Data outside the instrument's limit of detection (0.01–5.00 mg l^{-1}) were excluded from the calculations. Both observed and predicted TRP concentrations were log-transformed before calculating the statistics, and then converted back to normal values.

	Observed TRP (time-weighted)	Predicted TRP Diffuse P (flow-weighted)	Predicted TRP Diffuse + Point P (flow-weighted)
		mg l^{-1}	
lower limit (μ-1σ)	0.03	0.03	0.03
mean	0.06	0.08	0.08
upper limit (μ+1σ)	0.10	0.20	0.21
5th percentile	0.02	0.02	0.01
25th percentile	0.04	0.05	0.04
50th percentile	0.06	0.09	0.10
75th percentile	0.08	0.14	0.14
		Model A (Diffuse P)	**Model B (Diffuse + Point P)**
Percentage bias against distribution fitted to observations (%)	–	76	80

included when computing the final TRP concentration distribution prior to censoring it by instrument's limits of detection (0.01–5.00 mg l^{-1}), which may have skewed the model predictions. However, the model results are also skewed towards larger concentrations in the upper percentiles compared to the observations. The median modelled TRP concentration approximates the observed median, and as discussed, the tails of the modelled distributions are wider than those in observed mean daily data, which is also shown in Fig. 3.

Fig. 3 shows the overall model distributions compared to the lognormal distribution fitted to the observations. The boxplots and the density plots at their right-hand side show the full distributions excluding data points outside the instrument's limit of detection, while the dots scattered on top of the boxplots show only a sample (n = 30).

3.2.2. *Phosphorus concentrations in the stream – monthly performance*

Each month's modelled and observed TRP concentrations are shown as histogram plots in Fig. 4 A and as density plots in Fig. 4 B. The histograms show that the distributions from the simulations from both models approximate the peak of the distribution of the observations, however, the simulated concentration distributions have a lower tail that is not seen in the observed data. This discrepancy could be a product of how the predicted dissolved P concentration is being calculated in the model (see 3.2.1). The observations reported are aggregated daily mean values calculated from monitoring observations taken every 10-min. These daily means necessarily do not reflect the full range of concentration variability in the monitoring data, especially for extreme or short duration hydrological events, and they do not show diel P variations due to changes in temperature, light, and precipitation (Bieroza et al., 2023), which are likely to affect P mobilisation, delivery, and in-stream uptake. For example, see Table 3 for a comparison between the daily mean P and the 10-min P observations. Furthermore, the detection of low P concentrations is restricted by the instrument detection limits (0.01–5.00 mg l^{-1}). Although neither model reproduces the width of the observed data distributions, the simulated distributions from Model A are broader than those from Model B suggesting that Model B is marginally better

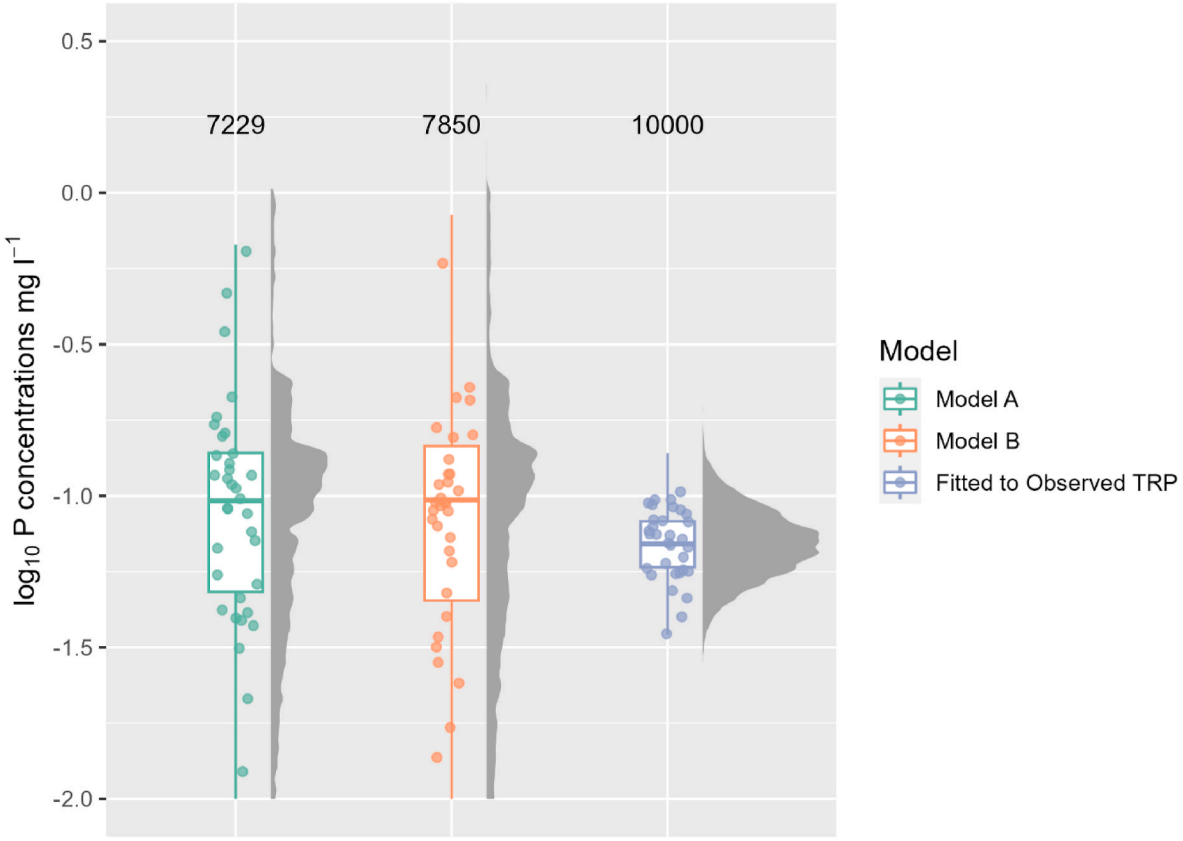

Fig. 3. Overall distribution density of log10 TRP concentrations fitted to observations versus those predicted by the two developed BBNs. BBN predictions show a larger variance, the full extent of which is shown in the plot by the density and box plots and scattered data points. Data outside the instrument's limit of detection (0.01–5.00 mg l^{-1}) were excluded from the plot, and the text shows the number of valid samples for each model. This plot was produced with the ggdist R package version 3.3.0 (Kay, 2023).

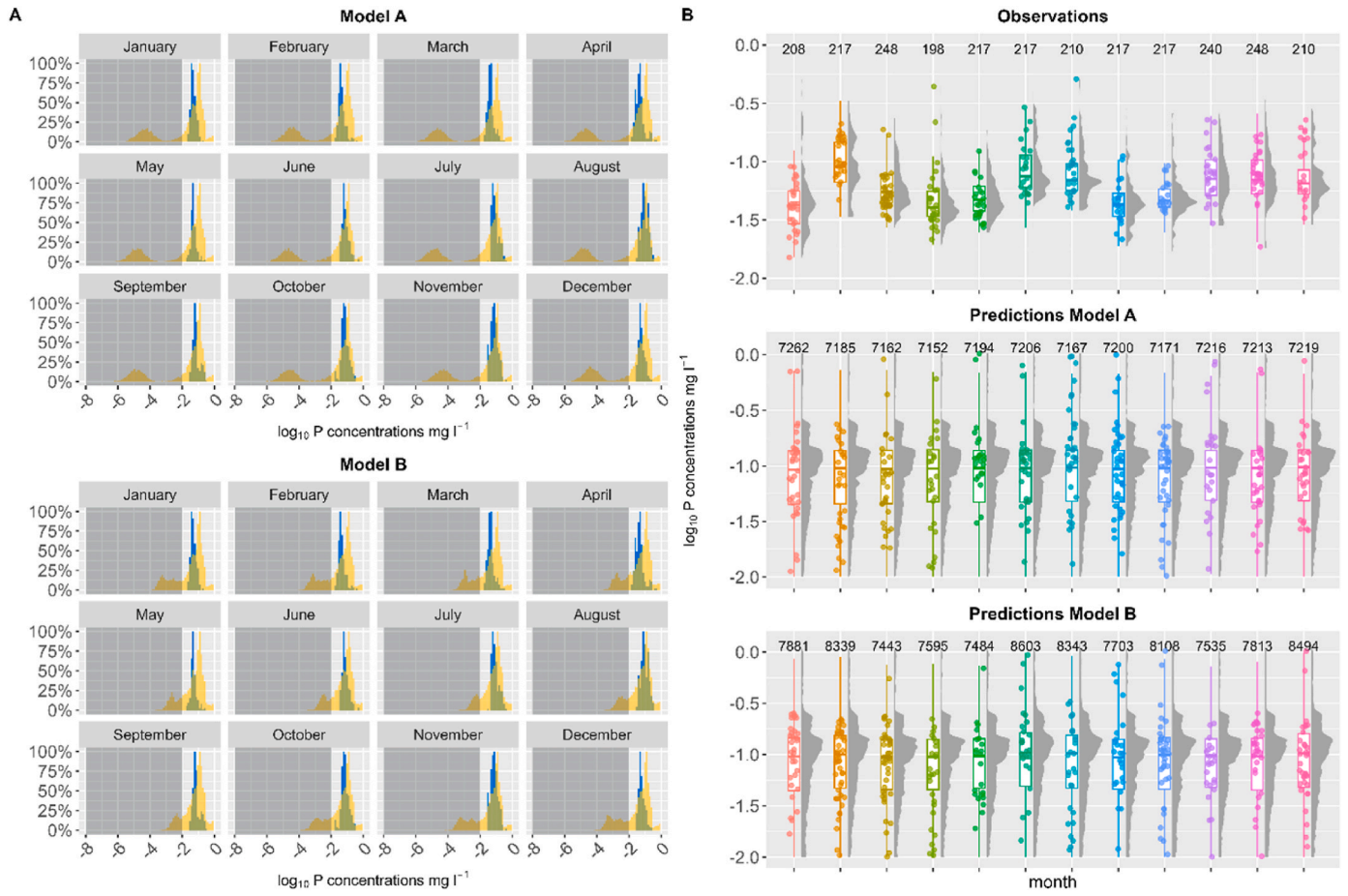

Fig. 4. A represents the histograms of each month's log10 of TRP concentrations (mg l^{-1}), observations are shown in blue, predictions obtained from the Diffuse P model (Model A, top figure) and Diffuse + Point P model (Model B, bottom figure) are shown in yellow. The histograms placed inside the grey box show values outside the limit of detection (0.01–5.00 mg l^{-1}). B represents the monthly density plots of log10 observations (top), the Diffuse P model (middle), and the Diffuse + Point P model (bottom). Data outside the instrument's limit of detection (0.01–5.00 mg l^{-1}) were excluded from the plots in box B, and the text shows the number of valid samples for each model. The density plots in box B were produced with the ggdist R package version 3.3.0 (Kay, 2023).

constrained. Importantly, the models predict flow-weighted concentrations (normalized by both time and discharge) rather than time-weighted (mean concentration in stream water as it passes the sampling point), which could in some cases better represent nutrient concentrations (i.e., for lakes, Rowland et al. (2021)). This may result in the different dilution effect in the model compared to the observations (see mean (μ) total discharge (Q, m^3), in Table 4). Monthly density plots show little to no seasonality, probably masked by model assumptions, which are further discussed in Table 5. Overall, the model represents the observed distribution between the 25th and 75th percentile very well, indicating strong predictive performance. This is especially notable when considering the small units (P concentrations) that are being reproduced and the complexities of processes affecting P dynamics in river catchments.

Table 4 summarizes each month's characteristics in terms of mean and median P concentrations, as well as mean discharge and model percentage bias calculated for the two BBNs. Percentage bias shows that the difference between the two models is minimal, corroborated by the nearly identical performance in terms of mean predicted concentrations. Mean total discharge (Q, m^3) is shown for Model B and the observations, assuming to be the same for Model A. The ratio between the modelled and the observed discharge shows how the models simulate 80–100% of flow correctly in most cases, except the summer months, when the modelled discharge is 60–70% of the observed. This underprediction can explain why the model average concentrations are higher than the observed ones (less discharge, less dilution).

3.2.3. *Phosphorus concentrations in the stream – risk of exceeding WFD standards*

For a speedy evaluation of the P loss risk, in-stream P concentrations were discretized according to the Environmental Quality Standard (EQS) for both models and evaluated against similarly discretized lognormal distribution fitted to the observed in-stream TRP. The EQS was classified as good (between 0 and 0.035 mg l^{-1}) and bad (above 0.035 mg l^{-1}), as 0.035 mg l^{-1} is the phosphate threshold established in Ireland to comply with the Water Framework Directive (European Communities Environmental Objectives (Surface Waters) European Communities Environmental Objectives Regulations, 2009). The comparison was done by censoring the concentrations for the instrument's limit of detection (0.01–5.00 mg l^{-1}). Overall, both models show a repartition good/bad threshold close to 40/60 % (data not shown), however, that is lower than the monthly EQS in the distribution fitted to the observations. The fitted observations agree with Mellander et al. (2022), who also showed that the probability of exceeding the EQS in this catchment was 93.7% of the time (data from 2010 to 2020). This discrepancy may be explained by the model's predicted TRP concentration distribution's inherent shape, which was left-skewed in comparison to the observed data, and by the censoring process, which might have caused a shift of the distribution towards 0.01 mg l^{-1}.

3.3. *Model strengths and limitations*

We designed a BBN to describe and calculate TRP losses at the

Table 3
Monitored TRP concentrations (mg l^{-1}) characteristics (correlation between the two datasets was 0.91). The two datasets have not been censored with the instrument's detection limits for this analysis, nor log-transformed.

	10-min concentration data	Daily mean concentration data
	mg l^{-1}	
Min	0.002	0.015
25th percentile	0.042	0.043
Median	0.057	0.058
75th percentile	0.082	0.085
Mean	0.075	0.075
Max	3.095	1.065

catchment outlet in a grassland-dominated Irish agricultural catchment. As compared to the steady-state probabilistic conceptual catchment model of P pollution risk by Glendell et al. (2022), the present model was parameterized using high-resolution datasets, including seven years of daily turbidity (NTU) and discharge (m^3) data at the catchment outlet, average soil Morgan P at field scale, and average measured farmyard size (instead of using a proxy of size). Using high-resolution turbidity data to calculate sediment losses at catchment outlet simplified the representation of erosion processes, thus avoiding assumptions regarding erosion rates, delivery, and the contribution of agricultural drains. Furthermore, the model was calibrated using seven years of daily observed TRP concentrations.

Model performance in terms of percentage bias (76–85% depending on which model version) was close to the 50% acceptable range recommended by Glendell et al. (2022), and appears small, given the small concentration values being simulated. Additionally, in terms of inter-quantile ranges, this BBN's performance approximates that of Glendell et al. (2022) BBN in the best performing catchments (Linkwood, Rough, and Lunan catchments) but is better constrained than the previous study's model in worse-performing catchments.

We offer an overview of the model assumption and subsequent potential limitations that we deem relevant in Table 5, highlighting several research gaps around P modelling in agricultural catchments. Specifically, there is still uncertainty around point sources, where weak priors from the literature were introduced due to a lack of monitoring data, as well as a simplification of soil P sources (Morgan P), which, albeit measured at high spatial resolution, were represented at discrete levels (indexes) used for monitoring, which may lead to loss of information. Table 5 also introduces the lack of in-stream biological P uptake, a process that could be significant in spring and summer, and could improve the model's representation of reality (Jackson-Blake et al., 2015). Lastly, a future enhancement to this study would be the use of a sensitivity analysis, which would improve understanding of which variables contribute the most to P losses at the catchment outlet. We note that the current method to implement a sensitivity analysis in GeNIe is only available for discrete BBNs. Discretization leads to a loss of information (Landuyt et al., 2013), and makes the sensitivity analysis dependent on the discretization method. In our case, a discretized network would not allow the calculation of quantiles from the model predictions for comparison with those from the observations, countering the utility of the high-frequency dataset used here. Thus, further work is required to implement a suitable sensitivity analysis methodology.

4. Conclusions

In this study, we combined different methodologies for using high-frequency water quality datasets to inform the priors of a BBN aimed at modelling P losses in Irish agricultural catchments. Different sources of P were introduced in the modelling exercise in a step-wise fashion, thus improving the model predictive ability and testing the model structural uncertainty. The two developed BBNs were able to predict the mean and median P concentrations in the stream well overall, with some limitations apparent in performance at the monthly time-step. However, the models' predictions presented wider distributions than the observations, which was noted in a similar work, and remains a property of this stochastic modelling approach. The BBN modelling approach allowed the inclusion of all the known P sources in the agricultural catchment, including farmyards, which is rare in P modelling, and septic tanks, which are often overlooked as P sources. In addition, this study directly reported on experts' role and selection as an effort to increase transparency. The probabilistic modelling highlighted the need for further targeted data collection to fill important knowledge gaps, even in a catchment with state-of-the-art high-resolution and long-term monitoring, such as the one used in this study. Furthermore, the work informed future research steps, which will include testing of model transferability, the influence of in-stream P cycling (i.e., estimation of removal by biota, and/or sediment uptake) on model performance, and understanding of P losses under future climate change scenarios.

Table 4
Summary of monthly characteristics and results, including model bias. Percentage bias and TRP concentrations have been calculated excluding data outside the instrument's limit of detection (0.01–5.00 mg l^{-1}). "A" columns show results for Model A and "B" columns show results for Model B. Both observed and predicted TRP concentrations were log-transformed before calculating the statistics, and then converted back to normal values.

	Percentage bias of simulations against distribution fitted to observed		mean (μ) concentrations (mg l^{-1})			median concentrations (mg l^{-1})			lower limit concentrations (μ-1σ) (mg l^{-1})			upper limit concentrations (μ+1σ) (mg l^{-1})			Mean total discharge (Q) m^3		
	A	B	A	B	obs	A	B	obs	A	B	obs	A	B	obs	Models	obs	model/observations ratio
Jan	69.4	74.5	0.08	0.08	0.05	0.09	0.10	0.04	0.03	0.03	0.03	0.20	0.21	0.07	9.99×10^5	11.0×10^5	0.9
Feb	74.5	70.9	0.08	0.08	0.04	0.09	0.09	0.04	0.03	0.03	0.03	0.21	0.20	0.07	7.42×10^5	7.48×10^5	1
Mar	67.5	70.7	0.08	0.08	0.04	0.09	0.09	0.04	0.03	0.03	0.03	0.20	0.20	0.07	4.07×10^5	4.83×10^5	0.8
Apr	69.9	77.9	0.08	0.08	0.05	0.09	0.09	0.04	0.03	0.03	0.03	0.20	0.21	0.09	2.73×10^5	3.06×10^5	0.9
May	69	81	0.08	0.08	0.05	0.10	0.10	0.05	0.03	0.03	0.02	0.20	0.22	0.07	2.03×10^5	2.28×10^5	0.9
Jun	73.5	89.2	0.08	0.09	0.07	0.10	0.10	0.07	0.03	0.03	0.03	0.20	0.23	0.13	1.40×10^5	2.24×10^5	0.6
Jul	70.3	101	0.08	0.09	0.09	0.09	0.10	0.07	0.03	0.03	0.05	0.20	0.24	0.14	0.85×10^5	1.15×10^5	0.7
Aug	68.5	89.1	0.08	0.09	0.09	0.09	0.10	0.09	0.03	0.03	0.05	0.20	0.23	0.16	1.51×10^5	2.52×10^5	0.6
Sept	76.5	95.6	0.09	0.09	0.07	0.10	0.10	0.06	0.04	0.03	0.04	0.21	0.24	0.12	1.05×10^5	1.03×10^5	1
Oct	72.2	73.8	0.08	0.08	0.07	0.10	0.09	0.07	0.03	0.03	0.04	0.2	0.21	0.13	3.94×10^5	4.41×10^5	0.9
Nov	73.8	71.8	0.09	0.08	0.07	0.10	0.10	0.07	0.03	0.03	0.04	0.21	0.21	0.12	9.10×10^5	9.83×10^5	0.9
Dec	73.8	72.5	0.08	0.08	0.06	0.09	0.09	0.05	0.03	0.03	0.04	0.20	0.20	0.09	10.10×10^5	11.20×10^5	0.9

Table 5
Model assumptions, limitations, and strengths.

Model assumptions	Consequences
Due to a lack of data, in-stream P removal by biota or sediment absorption is not represented.	In-stream P concentrations may be overestimated. However, these processes are secondary, especially considering the extreme flashiness of this catchment.
The main soil P source is spatially available at field resolution; however, the "Morgan P″ node was implemented using the categorical classification used in field monitoring.	The categorical variable "Morgan P″ can be used for testing management scenarios, however, discretization can lead to loss of information and impact decision making (Landuyt et al., 2013; Nojavan et al., 2017).
Amount of WEP transported to stream "Predicted Dissolved P Concentration" based on the equation for the closed period only, from the 15th of October to the 12th of January, when farmers are forbidden from spreading fertilizer on land in Ireland (Thomas et al., 2016b). The equation is applied to all months, and negative values are substituted with zeroes (see Table 1).	25% of the simulated values of this variable were zeroes, which probably skewed the in-stream concentration posterior distribution as discussed in section 3.2.1. This could be a contributing factor in the masking of seasonality in the model.
Experts noted that the septic tanks were modelled as a surface process, although soil risk classes have been included (Glendell et al., 2021), see variable "Soil risk factor" in section 2.4.	Might be underestimating P losses from STs.
P concentrations in septic tanks after primary or secondary treatment are based on (optimistic) Scottish EPA guidelines of Total P concentration reduction (Brownlie et al., 2014) even though the objective of the modelling was TRP.	There is uncertainty surrounding the actual TP/TRP concentration in a septic tank after primary or secondary treatment, and therefore more data is needed for this model compartment, as well as sensitivity testing.
Septic tanks were assumed to be working, no hypothesis was made regarding failure.	Might be underestimating P losses from STs.
There is no measured data for septic tank P concentration or loads, thus each month the load from septic tanks "Realised total load" is the same, as it is not dependent on discharge (Q).	Septic tank loads are not expected to vary seasonally; therefore, the model could be representing the domestic wastewater systems well, however, this could be one of the factors masking any seasonality in the model. However, septic tank loads have temporal patterns too, and are considered to be an important source of nutrients during spring and summer (Withers et al., 2014).
P concentrations from farmyards are modelled according to literature, however Moloney et al. (2020) found higher concentrations of TP in farmyard drains than that found by Harrison et al. (2019) (about 37 times).	Farmyard losses in the catchment cannot be estimated, and the uncertainty around these losses in the literature is very high, thus the model may be under or overestimating these losses. Further data collection is needed to test these assumptions.
The hydrology compartment, and consequently the rest of the model, was set up at a monthly time step.	This allows the integration of both sparse and high-resolution datasets, as well as the chance for future evaluation of management actions and mitigation measures. This also means that the model does not represent events and hot moments, which usually represent the larger contribution of P losses in a catchment, with climate change expected to increase their contribution (Ockenden et al., 2016).
Both models are calibrated and validated against daily averages of TRP concentration. The daily resolution data may not represent the full variability of the in-stream concentrations (statistics on the two datasets are shown in Table 3).	The model appears to simulate higher TRP concentrations in the upper quartiles than the observations (Table 2), but these may be realistic if compared against the sub-hourly dataset.

Ethics approval and consent to participate

All procedures performed and involving human participants were in accordance with the ethical standards and were reviewed and accepted by the Research Ethics Committee at the James Hutton Institute. Participants consented to provide their anonymized response. Care has been taken to ensure that information in the manuscript and Supporting material does not reveal participant identity or information.

CRediT authorship contribution statement

Camilla Negri: Conceptualization, Data curation, Formal analysis, Visualization, Writing – original draft, Writing – review & editing, Methodology. **Per-Erik Mellander:** Conceptualization, Data curation, Funding acquisition, Supervision, Writing – review & editing. **Nicholas Schurch:** Conceptualization, Methodology, Supervision, Writing – review & editing. **Andrew J. Wade:** Conceptualization, Funding acquisition, Supervision, Writing – review & editing. **Zisis Gagkas:** Methodology. **Douglas H. Wardell-Johnson:** Formal analysis. **Kerr Adams:** Methodology. **Miriam Glendell:** Conceptualization, Funding acquisition, Methodology, Project administration, Resources, Supervision, Writing – review & editing.

Declaration of competing interest

The authors declare that they have no known competing financial interests or personal relationships that could have appeared to influence the work reported in this paper.

Data availability

The datasets, models, code for the analysis and figures are available at https://github.com/CamillaNegri/Ballycanew_Ptool under the MIT license (https://github.com/git/git-scm.com/blob/main/MIT-LICENSE.txt).

Acknowledgements

We acknowledge the Teagasc Walsh Scholar Programme for providing the funding (Reference Number 2019021). We thank the experts for providing support in the model development as well as useful insights and directions, as well as the referees without whom the final draft of this paper would not have been possible. Last but not least, we wish to thank Orla Shortall, Evangelia Apostolakopoulou, and the whole the Research Ethics Committee at The James Hutton Institute; Edward Burgess, Mark Boland, Bridget Lynch, Una Cullen, and Simon Leach at the Teagasc Agricultural Catchments Programme for providing and explaining datasets, as well as giving context and insights on the catchments.

Supplementary data

Supplementary data to this article can be found online at https://doi.org/10.1016/j.envsoft.2024.106073.

Appendix A. catchment characteristics

Catchment characteristics

			Reference
General	**Location**	52°36′N, 6°20′W	Sherriff et al. (2015)
	Size	1191 ha	Teagasc - Agriculture and Food Development Authority, (2018)
	Median slope	3°	Sherriff et al. (2015)
	Altitude (m a.s.l.)	40–200	Mellander et al. (2015)
	Average field size (ha)	3.04	Thomas et al. (2016b)
Management	**Land use**	78% grassland, 20% tillage	Teagasc - Agriculture and Food Development Authority, (2018)
	Stocking rate (LU ha^{-1})	1.04	Sherriff et al. (2015)
Hydrology	**Soil series**	Typical Surface-water, Gleys or Groundwater, Gleys (71%), Typical Brown Earths (29%)	Thomas et al. (2016a)
	Drainage class	Poorly drained, well-drained in the uplands	Teagasc - Agriculture and Food Development Authority, (2018)
	Proportion of poorly drained soils on total area	85%	Shore et al. (2014)
	Dominant flow pathway	Surface	Thomas et al. (2016a)
	Stream order	2	Mellander et al. (2012)
	Runoff coefficient 2009–2014	0.48	Thomas et al. (2016b)
	Runoff flashiness (Q5:Q95)	202	Thomas et al. (2016b)
	Runoff Flashiness 2010–2020 (Q5/Q95)	126	Mellander et al. (2022)
	Ditch density (km^{2}km^{-2}) and area of channel network (% of catchment area)	1.3 (1.26%)	Shore et al. (2015)
	Channel density (%) per sediment retention class	Low (15%), low-moderate (10%), moderate-high (26%), high (49%)	Shore et al. (2015)
	Annual discharge 2010–2020 (mm yr^{-1})	1051	Mellander et al. (2022)
P loss	**Mean suspended sediment concentrations 2009–2012 (mg l^{-1})**	14	Sherriff et al. (2015)
	Mean suspended solids loads 2009–2012 (t km^{-2}yr^{-1})	26.64	Sherriff et al. (2015)
	Average P losses (kg TP ha^{-1}) 2010–2013	1.035	Mellander et al. (2015)
	Total Dissolved P (mg l^{-1}) ~ Total Reactive P (mg l^{-1}) at catchment outlet	TDP = 1.1475 × TRP + 0.0078	Shore et al. (2014)
	% areas at highest risk of legacy soil P transfers in baseline and (resampled) years with CSA Index threshold ≥ 5	5.6 (4.1)	Thomas et al. (2016b)
	Water Extractable P (WEP) ~ Soil Morgan P	WEP = 0.58 × SoilMorganP+1.13	Thomas et al. (2016b)
Connectivity	**Mean HSA size m^2 (% of catchment)[b]**	703,147 (6)	Thomas et al. (2016a)
	% hydrologically disconnected area over total catchment area[c]	24.9	Thomas et al. (2016a)

References

Aguilera, P.A., Fernández, A., Fernández, R., Rumí, R., Salmerón, A., 2011. Bayesian networks in environmental modelling. Environ. Model. Software 26, 1376–1388. https://doi.org/10.1016/j.envsoft.2011.06.004.

Barton, D.N., Kuikka, S., Varis, O., Uusitalo, L., Henriksen, H.J., Borsuk, M., de la Hera, A., Farmani, R., Johnson, S., Linnell, J.D., 2012. Bayesian networks in environmental and resource management. Integrated Environ. Assess. Manag. 8, 418–429. https://doi.org/10.1002/ieam.1327.

BayesFusion, 2019. GeNIe 2.4 [WWW Document]. https://www.bayesfusion.com/. (Accessed 5 June 2019).

Beven, K., 2019. Towards a methodology for testing models as hypotheses in the inexact sciences. Proc. R. Soc. Math. Phys. Eng. Sci. 475, 20180862 https://doi.org/10.1098/rspa.2018.0862.

Bieroza, M., Acharya, S., Benisch, J., ter Borg, R.N., Hallberg, L., Negri, C., Pruitt, A., Pucher, M., Saavedra, F., Staniszewska, K., van't Veen, S.G.M., Vincent, A., Winter, C., Basu, N.B., Jarvie, H.P., Kirchner, J.W., 2023. Advances in catchment science, hydrochemistry, and aquatic Ecology Enabled by high-frequency water quality measurements. Environ. Sci. Technol. https://doi.org/10.1021/acs.est.2c07798.

Blöschl, G., Bierkens, M.F.P., Chambel, A., 2019. Twenty-three unsolved problems in hydrology (UPH) – a community perspective. Hydrol. Sci. J. 64, 1141–1158. https://doi.org/10.1080/02626667.2019.1620507.

Bol, R., Gruau, G., Mellander, P.-E., Dupas, R., Bechmann, M., Skarbøvik, E., Bieroza, M., Djodjic, F., Glendell, M., Jordan, P., Van der Grift, B., Rode, M., Smolders, E., Verbeeck, M., Gu, S., Klumpp, E., Pohle, I., Fresne, M., Gascuel-Odoux, C., 2018. Challenges of reducing phosphorus based water eutrophication in the agricultural landscapes of Northwest Europe. Front. Mar. Sci. 5.

Borsuk, M.E., Stow, C.A., Reckhow, K.H., 2004. A Bayesian network of eutrophication models for synthesis, prediction, and uncertainty analysis. Ecol. Model. 173, 219–239. https://doi.org/10.1016/j.ecolmodel.2003.08.020.

Brazier, R.E., Heathwaite, A.L., Liu, S., 2005. Scaling issues relating to phosphorus transfer from land to water in agricultural catchments. J. Hydrol., Nutirent Mobility within River Basins: A European Perspective 304, 330–342. https://doi.org/10.1016/j.jhydrol.2004.07.047.

Brownlie, W., May, L., McDonald, C., Roaf, S., Spears, B.M., 2014. Assessment of a novel development policy for the control of phosphorus losses from private sewage systems to the Loch Leven catchment, Scotland, UK. Environ. Sci. Pol. 38, 207–216. https://doi.org/10.1016/j.envsci.2013.12.006.

Campbell, J.M., Jordan, P., Arnscheidt, J., 2015. Using high-resolution phosphorus data to investigate mitigation measures in headwater river catchments. Hydrol. Earth Syst. Sci. 19, 453–464. https://doi.org/10.5194/hess-19-453-2015.

Crockford, L., O'Riordain, S., Taylor, D., Melland, A., Shortle, G., Jordan, P., 2017. The application of high temporal resolution data in river catchment modelling and management strategies. Environ. Monit. Assess. 189, 461. https://doi.org/10.1007/s10661-017-6174-1.

Delignette-Muller, M.-L., Dutang, C., Pouillot, R., Denis, J.-B., Siberchiot, A., 2020. Package 'fitdistrplus': Help to Fit of a Parametric Distribution to Non-censored or Censored Data.

Djodjic, F., Markensten, H., 2019. From single fields to river basins: identification of critical source areas for erosion and phosphorus losses at high resolution. Ambio 48, 1129–1142. https://doi.org/10.1007/s13280-018-1134-8.

Environmental Protection Agency Ireland (EPA), 2015. National Inspection Plan: Domestic Waste Water Treatment Systems: Inspection Data Report 1st July 2013 – 31st December 2014. Johnstown Castle, Co, Wexford, 978-1-84095-615-3.
Environmental Protection Agency Ireland (EPA), 2003. A catchment based approach for reducing nutrient inputs from all sources to the lakes of Kilarney: final report. Lough Leane Catchment Monitoring and Management System. Kerry County Council, Ireland.
Environmental Protection Agency Ireland (EPA), 2000. Code of Practice: Wastewater Treatment Systems for Single Houses.
European Communities Environmental Objectives (Surface Waters) Regulations, 2009. Stationery Office, Dublin. S.I. No. 272 of 2009.
European Environment Agency, 2019. The European Environment: State and Outlook 2020 : Knowledge for Transition to a Sustainable Europe. Publications, Office, LU.
Forio, M.A.E., Landuyt, D., Bennetsen, E., Lock, K., Nguyen, T.H.T., Ambarita, M.N.D., Musonge, P.L.S., Boets, P., Everaert, G., Dominguez-Granda, L., Goethals, P.L.M., 2015. Bayesian belief network models to analyse and predict ecological water quality in rivers. Ecol. Model. 312, 222–238. https://doi.org/10.1016/j.ecolmodel.2015.05.025.
Gill, L., 2005. Ireland, environmental protection agency, environmental research technological development and innovation Programme. Water Framework Directive: an Investigation into the Performance of Subsoils and Stratified Sand Filters for the Treatment of Wastewater from On-Site Systems (2001-MS-15-M1) : Synthesis Report. Environmental Protection Agency, Johnstown Castle, Co. Wexford.
Gill, L.W., Mockler, E.M., 2016. Modeling the pathways and attenuation of nutrients from domestic wastewater treatment systems at a catchment scale. Environ. Model. Software 84, 363–377. https://doi.org/10.1016/j.envsoft.2016.07.006.
Gill, L.W., O'Súlleabháin, C., Misstear, B.D.R., Johnston, P.J., 2007. The treatment performance of different subsoils in Ireland receiving on-site wastewater effluent. J. Environ. Qual. 36, 1843–1855. https://doi.org/10.2134/jeq2007.0064.
Glendell, M., Gagkas, Z., Richards, S., Halliday, S., 2021. Developing a Probabilistic Model to Estimate Phosphorus, Nitrogen and Microbial Pollution to Water from Septic Tanks. Scotland's Centre of Expertise for Waters (CREW).
Glendell, M., Gagkas, Z., Stutter, M., Richards, S., Lilly, A., Vinten, A., Coull, M., 2022. A systems approach to modelling phosphorus pollution risk in Scottish rivers using a spatial Bayesian Belief Network helps targeting effective mitigation measures. Front. Environ. Sci. 10.
Glendell, M., Palarea-Albaladejo, J., Pohle, I., Marrero, S., McCreadie, B., Cameron, G., Stutter, M., 2019. Modeling the ecological impact of phosphorus in catchments with multiple environmental stressors. J. Environ. Qual. 48, 1336–1346. https://doi.org/10.2134/jeq2019.05.0195.
Harris, G.P., Heathwaite, A.L., 2012. Why is achieving good ecological outcomes in rivers so difficult? Freshw. Biol. 57, 91–107. https://doi.org/10.1111/j.1365-2427.2011.02640.x.
Harrison, S., McAree, C., Mulville, W., Sullivan, T., 2019. The problem of agricultural 'diffuse' pollution: getting to the point. Sci. Total Environ. 677, 700–717. https://doi.org/10.1016/j.scitotenv.2019.04.169.
Haygarth, P.M., Condron, L.M., Heathwaite, A.L., Turner, B.L., Harris, G.P., 2005. The phosphorus transfer continuum: linking source to impact with an interdisciplinary and multi-scaled approach. Sci. Total Environ. 344, 5–14. https://doi.org/10.1016/j.scitotenv.2005.02.001.
Jackson-Blake, L., Wade, A., Futter, M., Butterfield, D., Couture, R.-M., Cox, B., Crossman, J., Ekholm, P., Halliday, S., Jin, L., Lawrence, D.S.L., Lepistö, A., Lin, Y., Rankinen, K., Whitehead, P., 2016. The INtegrated CAtchment model of phosphorus dynamics (INCA-P): description and demonstration of new model structure and equations. Environ. Model. Software 83, 356–386. https://doi.org/10.1016/j.envsoft.2016.05.022.
Jackson-Blake, L.A., Dunn, S.M., Helliwell, R.C., Skeffington, R.A., Stutter, M.I., Wade, A. J., 2015. How well can we model stream phosphorus concentrations in agricultural catchments? Environ. Model. Software 64, 31–46. https://doi.org/10.1016/j.envsoft.2014.11.002.
Jackson-Blake, L.A., Sample, J.E., Wade, A.J., Helliwell, R.C., Skeffington, R.A., 2017. Are our dynamic water quality models too complex? A comparison of a new parsimonious phosphorus model, SimplyP, and INCA-P: over-complexity in water quality models. Water Resour. Res. 53, 5382–5399. https://doi.org/10.1002/2016WR020132.
Jarvie, H.P., Sharpley, A.N., Flaten, D., Kleinman, P.J.A., 2019. Phosphorus mirabilis: illuminating the past and future of phosphorus stewardship. J. Environ. Qual. 48, 1127–1132. https://doi.org/10.2134/jeq2019.07.0266.
Jordan, P., Arnscheidt, A., McGrogan, H., McCormick, S., 2007. Characterising phosphorus transfers in rural catchments using a continuous bank-side analyser. Hydrol. Earth Syst. Sci. 11, 372–381. https://doi.org/10.5194/hess-11-372-2007.
Kaikkonen, L., Parviainen, T., Rahikainen, M., Uusitalo, L., Lehikoinen, A., 2021. Bayesian networks in environmental risk assessment: a review. Integrated Environ. Assess. Manag. 17, 62–78. https://doi.org/10.1002/ieam.4332.
Kay, M., 2023. {ggdist}: Visualizations of Distributions and Uncertainty.
Kragt, M.E., 2009. A beginners guide to Bayesian network modelling for integrated catchment management. Landscape Logic. Technical Report No. 9.
Landuyt, D., Broekx, S., D'hondt, R., Engelen, G., Aertsens, J., Goethals, P.L.M., 2013. A review of Bayesian belief networks in ecosystem service modelling. Environ. Model. Software 46, 1–11. https://doi.org/10.1016/j.envsoft.2013.03.011.
Mellander, P.-E., Galloway, J., Hawtree, D., 2022. Phosphorus mobilization and delivery estimated from long-term high frequency water quality and discharge data. Front. Water 4. https://doi.org/10.3389/frwa.2022.917813.
Mellander, P.-E., Jordan, P., Bechmann, M., Fovet, O., Shore, M.M., McDonald, N.T., Gascuel-Odoux, C., 2018. Integrated climate-chemical indicators of diffuse pollution from land to water. Sci. Rep. 8, 1–10. https://doi.org/10.1038/s41598-018-19143-1.
Mellander, P.-E., Jordan, P., Shore, M., Melland, A.R., Shortle, G., 2015. Flow paths and phosphorus transfer pathways in two agricultural streams with contrasting flow controls. Hydrol. Process. 29, 3504–3518. https://doi.org/10.1002/hyp.10415.
Mellander, P.-E., Melland, A.R., Jordan, P., Wall, D.P., Murphy, P.N.C., Shortle, G., 2012. Quantifying nutrient transfer pathways in agricultural catchments using high temporal resolution data. Environ. Sci. Policy, CATCHMENT SCIENCE AND POLICY EVALUATION FOR AGRICULTURE AND WATER QUALITY 24, 44–57. https://doi.org/10.1016/j.envsci.2012.06.004.
Mockler, E.M., Deakin, J., Archbold, M., Daly, D., Bruen, M., 2016. Nutrient load apportionment to support the identification of appropriate water framework directive measures. Biol. Environ. 116B, 245–263. https://doi.org/10.3318/bioe.2016.22.
Mockler, E.M., Deakin, J., Archbold, M., Gill, L., Daly, D., Bruen, M., 2017. Sources of nitrogen and phosphorus emissions to Irish rivers and coastal waters: estimates from a nutrient load apportionment framework. Sci. Total Environ. 601–602, 326–339. https://doi.org/10.1016/j.scitotenv.2017.05.186.
Moe, S.J., Carriger, J.F., Glendell, M., 2021. Increased use of bayesian network models has improved environmental risk assessments. Integrated Environ. Assess. Manag. 17, 53–61. https://doi.org/10.1002/ieam.4369.
Moloney, T., Fenton, O., Daly, K., 2020. Ranking connectivity risk for phosphorus loss along agricultural drainage ditches. Sci. Total Environ. 703, 134556 https://doi.org/10.1016/j.scitotenv.2019.134556.
Nojavan, F., Qian, S.S., Stow, C.A., 2017. Comparative analysis of discretization methods in Bayesian networks. Environ. Model. Software 87, 64–71. https://doi.org/10.1016/j.envsoft.2016.10.007.
Oakley, J., 2020. SHELF: Tools to Support the Sheffield Elicitation Framework.
Ockenden, M.C., Deasy, C.E., Benskin, C.McW.H., Beven, K.J., Burke, S., Collins, A.L., Evans, R., Falloon, P.D., Forber, K.J., Hiscock, K.M., Hollaway, M.J., Kahana, R., Macleod, C.J.A., Reaney, S.M., Snell, M.A., Villamizar, M.L., Wearing, C., Withers, P. J.A., Zhou, J.G., Haygarth, P.M., 2016. Changing climate and nutrient transfers: evidence from high temporal resolution concentration-flow dynamics in headwater catchments. Sci. Total Environ. 548–549, 325–339. https://doi.org/10.1016/j.scitotenv.2015.12.086.
Packham, I., Mockler, E., Archbold, M., Mannix, A., Daly, D., Deakin, J., Bruen, M., 2020. Catchment characterisation tool: prioritising critical source areas for managing diffuse nitrate pollution. Environ. Model. Assess. 25, 23–39. https://doi.org/10.1007/s10666-019-09683-9.
Pappenberger, F., Beven, K.J., 2006. Ignorance is bliss: or seven reasons not to use uncertainty analysis. Water Resour. Res. 42 https://doi.org/10.1029/2005WR004820.
Penk, M.R., Bruen, M., Feld, C.K., Piggott, J.J., Christie, M., Bullock, C., Kelly-Quinn, M., 2022. Using weighted expert judgement and nonlinear data analysis to improve Bayesian belief network models for riverine ecosystem services. Sci. Total Environ. 851, 158065 https://doi.org/10.1016/j.scitotenv.2022.158065.
Phan, T.D., Smart, J.C.R., Stewart-Koster, B., Sahin, O., Hadwen, W.L., Dinh, L.T., Tahmasbian, I., Capon, S.J., 2019. Applications of bayesian networks as decision support tools for water resource management under climate change and socio-economic stressors: a critical appraisal. Water 11, 2642. https://doi.org/10.3390/w11122642.
Radcliffe, D.E., Freer, J., Schoumans, O., 2009. Diffuse phosphorus models in the United States and europe: their usages, scales, and uncertainties. J. Environ. Qual. 38, 1956–1967. https://doi.org/10.2134/jeq2008.0060.
Regan, J., Fenton, O., Healy, M., 2012. A review of phosphorus and sediment release from Irish tillage soils, the methods used to quantify losses and the current state of mitigation practice. Biol. Environ. 112, 157–183. https://doi.org/10.3318/BIOE.2012.05.
Rode, M., Arhonditsis, G., Balin, D., Kebede, T., Krysanova, V., Griensven, A. vanZee, van der, S.E.A.T.M., 2010. New challenges in integrated water quality modelling. Hydrol. Process. 24, 3447–3461. https://doi.org/10.1002/hyp.7766.
Rowland, F.E., Stow, C.A., Johnson, L.T., Hirsch, R.M., 2021. Lake Erie tributary nutrient trend evaluation: normalizing concentrations and loads to reduce flow variability. Ecol. Indicat. 125, 107601 https://doi.org/10.1016/j.ecolind.2021.107601.
Sahlin, U., Helle, I., Perepolkin, D., 2021. "This is what we don't know": treating epistemic uncertainty in bayesian networks for risk assessment. Integrated Environ. Assess. Manag. 17, 221–232. https://doi.org/10.1002/ieam.4367.
Schulte, R.P.O., Melland, A.R., Fenton, O., Herlihy, M., Richards, K., Jordan, P., 2010. Modelling soil phosphorus decline: expectations of water framework directive policies. Environ. Sci. Pol. 13, 472–484. https://doi.org/10.1016/j.envsci.2010.06.002.
Sherriff, S., Rowan, J.S., Fenton, O., Jordan, P., Melland, A.R., Mellander, P.-E., hUallacháin, D.Ó., 2016. Storm Event Suspended Sediment-Discharge Hysteresis and Controls in Agricultural Watersheds: Implications for Watershed Scale Sediment Management. Environ. Sci. Technol. 50, 1769–1778. https://doi.org/10.1021/acs.est.5b04573.
Sherriff, S., Rowan, J.S., Melland, A.R., Jordan, P., Fenton, O., Ó hUallacháin, D., 2015. Investigating suspended sediment dynamics in contrasting agricultural catchments using ex situ turbidity-based suspended sediment monitoring. Hydrol. Earth Syst. Sci. 19, 3349–3363. https://doi.org/10.5194/hess-19-3349-2015.
Shore, M., Jordan, P., Mellander, P.-E., Kelly-Quinn, M., Daly, K., Sims, J.T., Wall, D.P., Melland, A.R., 2016. Characterisation of agricultural drainage ditch sediments along the phosphorus transfer continuum in two contrasting headwater catchments. J. Soils Sediments 16, 1643–1654. https://doi.org/10.1007/s11368-015-1330-0.
Shore, M., Jordan, P., Mellander, P.-E., Kelly-Quinn, M., Melland, A.R., 2015. An agricultural drainage channel classification system for phosphorus management.

Agric. Ecosyst. Environ. 199, 207–215. https://doi.org/10.1016/j.agee.2014.09.003.

Shore, M., Jordan, P., Mellander, P.-E., Kelly-Quinn, M., Wall, D.P., Murphy, P.N.C., Melland, A.R., 2014. Evaluating the critical source area concept of phosphorus loss from soils to water-bodies in agricultural catchments. Sci. Total Environ. 490, 405–415. https://doi.org/10.1016/j.scitotenv.2014.04.122.

Stutter, M., Barros Costa, F., O Huallachain, D., 2021. Riparian buffer zone quantitative effectiveness review database 3. https://doi.org/10.17632/t64dbpv63x.3.

Teagasc - Agriculture and Food Development Authority, 2018. Agricultural Catchments Programme - Phase 2 Report, https://www.teagasc.ie/publications/2018/agricultural-catchments-programme—phase-2-report.php.

Thomas, I.A., Bruen, M., Mockler, E., Werner, C., Mellander, P.-E., Reaney, S., Rymszewicz, A., McGrath, G., Eder, E., Wade, A.J., Collins, A., Arheimer, B., 2021. Catchment models and management tools for diffuse contaminants (sediment, phosphorus and pesticides): DiffuseTools Project (No. 396). ENVIRONMENTAL PROTECTION AGENCY An Ghníomhaireacht um Chaomhnú Comhshaoil PO Box 3000. Johnstown Castle, Co. Wexford, Ireland.

Thomas, I.A., Jordan, P., Mellander, P.-E., Fenton, O., Shine, O., Ó hUallacháin, D., Creamer, R., McDonald, N.T., Dunlop, P., Murphy, P.N.C., 2016a. Improving the identification of hydrologically sensitive areas using LiDAR DEMs for the delineation and mitigation of critical source areas of diffuse pollution. Sci. Total Environ. 556, 276–290. https://doi.org/10.1016/j.scitotenv.2016.02.183.

Thomas, I.A., Mellander, P.-E., Murphy, P.N.C., Fenton, O., Shine, O., Djodjic, F., Dunlop, P., Jordan, P., 2016b. A sub-field scale critical source area index for legacy phosphorus management using high resolution data. Agric. Ecosyst. Environ. 233, 238–252. https://doi.org/10.1016/j.agee.2016.09.012.

Uusitalo, L., 2007. Advantages and challenges of Bayesian networks in environmental modelling. Ecol. Model. 203, 312–318. https://doi.org/10.1016/j.ecolmodel.2006.11.033.

Vero, S.E., Daly, K., McDonald, N.T., Leach, S., Sherriff, S., Mellander, P.-E., 2019. Sources and mechanisms of low-flow river phosphorus elevations: a repeated synoptic survey approach. Water 11, 1497. https://doi.org/10.3390/w11071497.

Wade, A.J., Jackson, B.M., Butterfield, D., 2008. Over-parameterised, uncertain 'mathematical marionettes' — how can we best use catchment water quality models? An example of an 80-year catchment-scale nutrient balance. Sci. Total Environ. 400, 52–74. https://doi.org/10.1016/j.scitotenv.2008.04.030.

Wall, D., Jordan, P., Melland, A.R., Mellander, P.-E., Buckley, C., Reaney, S.M., Shortle, G., 2011. Using the nutrient transfer continuum concept to evaluate the European union nitrates directive national action Programme. Environ. Sci. Pol. 14, 664–674. https://doi.org/10.1016/j.envsci.2011.05.003.

Wall, D.P., Murphy, P.N.C., Melland, A.R., Mechan, S., Shine, O., Buckley, C., Mellander, P.-E., Shortle, G., Jordan, P., 2012. Evaluating nutrient source regulations at different scales in five agricultural catchments. Environ. Sci. Pol. 24, 34–43. https://doi.org/10.1016/j.envsci.2012.06.007.

Wellen, C., Kamran-Disfani, A.-R., Arhonditsis, G.B., 2015. Evaluation of the current state of distributed watershed nutrient water quality modeling. Environ. Sci. Technol. 49, 3278–3290. https://doi.org/10.1021/es5049557.

Withers, P.J., Jordan, P., May, L., Jarvie, H.P., Deal, N.E., 2014. Do septic tank systems pose a hidden threat to water quality? Front. Ecol. Environ. 12, 123–130. https://doi.org/10.1890/130131.

Zambrano-Bigiarini, M., 2020. hydroGOF: goodness-of-fit functions for comparison of simulated and observed hydrological time series. https://doi.org/10.5281/zenodo.839854.